Basrah Journal for Engineering Sciences, Vol. 23, No. 2, (2023), 58-71

Original Article

Journal homepage: www.bjes.edu.iq
ISSN (Online): 23118385, ISSN (Print): 18146120

OPEN ACCESS

Experimental Study of the Effect of Wire Electrical Discharge Machining on Crack tip Opening Displacement for Compact Tension Specimens of Low Carbon Steel

Sara A. Khudair [1, *], Atheed H. Taha [2], Ameen A. Nassar [3]

[1,2,3] *Department of Mechanical Engineering, College of Engineering, University of Basrah, Basrah, Iraq*
E-mail addresses: sarakhdhierl@gmail.com, atheed.taha@uobasrah.edu.iq, aaledanil@gmail.com

Received: 15 December 2022; Accepted: 5 February 2023; Published: 30 December 2023

Abstract

Fracture mechanics approach is important for all mechanical and civil projects that might involve cracks in metallic materials the purpose of this paper is to determine a crack tip opening displacement fracture toughness experimentally, also study the effect of thickness on CTOD fracture toughness of low carbon steel and study the effect of Wire Electrical Discharge Machine (WEDM) to have a pre-crack, instead of fatigue pre-crack by using a CT specimen of low carbon steel with a thickness of (8,10, and15 mm), a width of 30mm, crack length of 15mm, and pre-crack of 1.3mm for all samples, this dimension according to ASTM-E399-13, by pulling the specimen in a 100 KN universal testing machine at a slow speed rate of 0.5 mm/min, the load applied on the specimen is generally a tension load. The crack tip plastically deforms until a critical point P_C at this moment a crack is initiated. The computer-controlled universal testing machine gives the value of the load and the displacement transducer gives a crack mouth opening displacement. Critical crack tip opening displacement CTOD is found with the plastic hinge model (PHM) method. The result showed the stress intensity factor K_I increases with increased loading in the elastic region and the thickness effect refers to the effect of the plastic zone at the crack tip on the stress intensity factor, In a thin specimen, a plastic zone is large at the fracture tip leads to a high-stress intensity factor at the fracture tip but in the thick specimen, on the other hand, has a small a plastic zone and a low-stress intensity factor around the crack tip. The fracture toughness is found to increase with an increase in the thickness of specimens.

Keywords: CTOD, WEDM, Low carbon steel, CFOA, EPFM

https://doi.org/10.33971/bjes.23.2.8

1. Introduction

Fundamental concepts of fracture mechanics can be traced back to the late nineteenth and early twentieth centuries. Both experimental observations and theoretical elasticity contributed the creation of the fundamental aspects of the theory of fracture mechanics[1].

Many factors contribute to the failure of an engineering component, i.e. flaw or inclusion in material, cyclic fatigue loading, and residual stresses in the material. One of the most notable failure cases in history is the brittle fracture of Liberty Ships in the 1940s, where 1031 of 2078 ships experienced brittle-related damage. The lack of understanding of fracture at the time did not recognize material strength at low temperatures and the effects due to weld-ments, which led to an expensive lesson in fracture. This incident led to more research in fracture mechanics.

Fracture mechanics is a study of the material's fracture resistivity, consisting of two main parts; linear elastic fracture mechanics (LEFM) and elastic-plastic fracture mechanics (EPFM). Linear elastic fracture mechanics describes the material's fracture resistance within the elastic yielding region, mainly represented by stress intensity factor K_I Stress intensity factor (SIF) is the most important single parameter in fracture mechanics, which can be used to examine if a crack would propagate in a cracked structure

under particular loading condition[2], the elastic-plastic fracture mechanics considers post yielding where the crack deforms plastically, represented by the J-integral and crack tip opening displacement, CTOD [3].In fracture mechanics, when the stress intensity factor in the crack tip is equal to the material fracture toughness, a crack will start to grow. That means the fracture toughness of a material can forecast the remaining strength of a component with an initial crack. Although fracture toughness is a material inherent attribute, for the same material, different fracture toughness values were determined in different tests as test conditions (temperature, loading rate, et al) and specimen size are different. Of all the influence factors for fracture toughness tests, specimen thickness is the most important factor. Stress in crack tip varies as pipe thickness is different. As thickness increases, a stress-strain field in the crack tip starts changing to a plane strain state from a plane stress state, which means the crack tip is in a tension state in all three directions and the plastic zone will be limited in a small scope. So critical fracture toughness will decreases when pipe thickness

increases in the plane strain state, and brittle fracture is prone to happen, which is much more dangerous compared with a ductile fracture [4].

Fatigue pre-cracking is always preferred for the pre-cracking process on test samples for fracture tests. However, it is observed that specimens are damaged during the fatigue pre-cracking process as the crack direction is changed because of vibrations in a machine and the fixture holding the specimen. It is also observed that the fatigue pre-cracking induces residual plastic stresses. Such samples may produce wrong results on fracture toughness. The fatigue pre-cracking is a time-consuming process as well. The other option wire electric discharge machine (WEDM) is extensively used with the least wire diameter for pre-cracking. WEDM produces notched specimens[5]

The CTOD fracture toughness and effect of WEDM on fracture toughness have been the subject of several studies some of these were experimental and others works or numerical works.

Panontin, et al. 2000 [6] Improved formulae for estimating crack tip opening displacement (CTOD) from test records of compact tension CT specimens are developed. Two-dimensional, plane strain, finite element analyses of CT specimens are made for normalized crack depths, (a/W) of (0.40- 0.70) using Ramberg-Osgood material behavior. Finite element predictions of J, CTOD, crack mouth opening displacement CMOD and load is used to obtain proportionality constants relating the area under the load_ $CMOD_{pl}$ curve to J_{pl}, and J to CTOD in terms of (a/W), and Improvements in CTOD estimates of 25% over existing estimation methods are obtained. Correction factors for displacements measured on the specimen front face instead of the load line are also examined.

Kulkarn, et al. (2002)[7] Present an investigation of determining a critical value CTOD and fracture toughness in sheet metals. The Finite Element Analysis approach was used for a crack-tip opening displacement CTOD computed for sheets of Deep and Extra Deep-Drawn (EDD) steel compact tension specimens with three dimensions to support the findings on various fracture parameters. Four specimens were examined, with a thickness of 1.18, 1.38, 1.64, and 1.69 mm. Estimation critical crack tip opening displacement ($CTOD_C$) is divided into two parts elastic part and plastic part. They used the dug dual model to estimate the elastic component of CTOD under conditions of plane strain, and they used the plastic hinge model to estimate the plastic component. The result indicates that the change of critical $CTOD_C$ and the relationship between equivalent fracture toughness (K_Q) and sheet thickness that both experimental findings and FE values are in good agreement (within 1-4%) and with an increase in thickness, fracture toughness rises.

Kudari and Kodancha (2008) [8] Used ANSYS PROGRAM to estimate the magnitude of a crack tip opening displacement CTOD by a plastic hinge model by using compact tension CT & Single Edge Notched Bending SENB specimens which were prepared according to ASTM-E1290. They created finite element meshes for these specimens employing eight-node Iso-parametric elements for one-half of the specimens using 2-D analysis. The results indicate that the relation between J and CTOD is linear and heavily dependent on the technique of estimating CTOD, specimen shape, and specimen (a/w) ratio.

Kulkarn, et al. (2008) [9] Studied the effect of the thickness on fracture toughness for Extra Deep Drawn (EDD) steel compact tension specimens. For the fracture test, the rate of 0.2 mm/min was employed. Load-line displacement is measured using a gauge CMOD. The estimation Critical value of Crack Tip Opening Displacement ($CTOD_C$) had divided into elastic and plastic parts, Dug Dale's model is used to estimate the elastic component, and the plastic component is derived using the Plastic Hinge Model (PHM), the Crack Flank Opening Angle (CFOA), and the Finite Element Model (FEM). In the case of the EDD sheet of steel, severe deformation had been detected around the crack tips, leading to a larger value of plastic load displacement. Experimental studies show that thickness affects fracture toughness, high shear lip degree, also a large plastic zone, all the above reasons (defects) leads to the dominance of the plane stress condition, also it is determined that the proposed CFOA model is appropriate for high CTOD values.

Chaudhari, et al. (2009) [5] Investigation conducted to establish the influence of notch radius (ρ) on crack tip opening displacement CTOD according to standard ASTM E1290-89 measures are performed on Extra Deep Drawn EDD steel compact tension specimens that have pre-cracking by WEDM and notch root radius values ranging from 0.07 to 0.75 mm. The critical value of the crack tip opening displacement $CTOD_C$ consists of two-part; plastic and elastic parts, the elastic part had determined by Kanninen solution where he had used Dug-dale`s model, but the plastic part is by the crack flank opening angle (CFOA) method. Experimental results of CTOD for different notch radii illustrate that CTOD changes according to the change in a notch radius ρ from 0.07 to 0.75 and that there is a 0.93% improvement in the range of notch radiuses in fracture toughness of 0.07 mm to 0.15 mm. Otherwise, there is a significant improvement in toughness to fracture in the notch radius range from 0.15 to 0.75 mm. As a result, a critical notch radius is 0.15 mm, below this notch radius, is almost completely independent of fracture toughness. The area of plastic grows incrementally with a notch radius and increases in the magnitude of blunting up to 0.15 mm, there is hardly an enlargement of the plastic zone. The results presented an agreement with previous research for a ductile material. A high value of notch radius with a low thick steel sheet leads to more plasticity because of the full degree of shear-lip, high formability, material constraint, smaller sheet size, and the large plastic zone of EDD sheets, than the notch radius is lower than crack tip opening displacement CTOD.

Madyira, (2015) [10] Study the effect of Wire Electrical Discharge Machining (WEDM) on fracturing toughness. The important aim was to measure if the WEDM could be used conversely to generate a pre-crack by fatigue technique into an aluminum 7075-T6511 CT specimen following an ASTME-1820-11 standard. Four specimens were fracture tested after being pre-cracked using the WEDM process. The investigation results were discovered to be incompatible with theoretical estimates. The WEDM caused a Heat Affected Zone (HAZ) on the pre-crack surface that influence the material's fracture behavior. WEDM was shown to be an unsuccessful technique during the experiment, the average K_{IC} value which is lower than the literature with error 35%.

Avila, et al. (2016) [11] Studied the crack tip opening displacement based on standard ASTM E1290 using a single-edge notched SE bending sample. The result obtained from the effects of the crack tip opening displacement is dependent

on many factors as well including sample thickness and geometry, load, etc. Thickness affects the toughness of the fracture, especially in the area of transformation from a flattened fracture to a fragile fracture, as well as the durability increases with the increase in thickness. As a result, utilizing thin specimens to evaluate fracture toughness in that location is dangerous and also showed that the wire method could be considered a good method because it did not show any effect on the tip of the notch.

Sołtysiak, et al. (2016) [12] present a comparative analysis of the crack length "a" as a function of a crack-opening displacement "δ" obtained by experimental and numerical methods. The tests were performed under ambient temperature for CT-type specimens made of Ti6Al4V titanium alloy. Numerical research was carried out by finite element method using ABAQUS software. Satisfactory results were obtained which gave the reasons for establishing a hybrid method for the crack length determination.

Heidarvand et al. (2017) [13] Measured the fracture toughness of aluminum sheets using tensile stress tests and the finite element method with ABAQUS software. Linear Fracture Mechanics (LFM) and Feddersen`s approach had used in calculating the intensity factor (K_I) of samples with central wire-cut cracks and fatigue cracks of various sizes. There was just a 9% difference according to a fatigue-cracked sample. On one-quarter of the material, finite element analysis was done with both singular Borsum and regular iso-parametric elements. There was also a little variation between the findings produced by the finite element approach utilizing singular elements and the experimental findings. Although the SIF obtained by using the fatigue approach is more accurate than the value obtained by using wire-cut but where extremely high precision is not necessary, wire-cut cracks can be employed as an alternative for SIF calculation with acceptable accuracy.

Abdulsada (2018) [14] Introduced studying experimentally some mechanical properties, stress intensity factor, and the crack mouth opening displacement CMOD for the base and welded low carbon steel metal using single edge crack tension SECT, using the capabilities of Finite Element ABAQUS software and the Extended Finite Element Method (XFEM) capabilities to determine the numerical results of the tensile test for 3D single edge crack tension SECT specimens. Finally, the numerical results are compared with the results of the experiment, and the simulated findings and experimental results did not differ significantly.

Ahamed et al. (2019) [15] Investigated of mechanical and tribological properties of Aluminium 7075 reinforced with various weight % (3, 6, 9and 12)ZrSiO4. The specimens assess to evaluate fracture toughness (K_{1c}) were single-edge notch bending (SENB). To produce a notch on the SENB specimen, a CNC wire cut (EDM) molybdenum wire with a diameter of 0.18mm is employed. This specimen has been manufactured following ASTM E-399 standards. After the specimen has been pre-cracked, a load is applied in the middle of the specimen as the 3-point bending load, and the extensometer connected will measure the (COD) crack opening displacement. The Test specimens show valid results by satisfying all the required condition, experimental analysis of Maximum fracture toughness (K_{max}) is 23.63 and critical fracture toughness (K_{1c}) is 22.67 obtained for 9% weight of ZrSiO4. Analytical results shows Maximum fracture toughness (K_{max}) is 23.40 and critical fracture toughness (K_{1c}) is 22.15 has obtained for 9% weight of ZrSiO4. For all test specimens, the experimental and analytical results are equivalent.

Nassar and Fayyad (2019) [16] Determined the fracture toughness of the elastic stage by the ANSYS SOFTWARE following ASTM-E-399. However, in the elastic-plastic region, the crack tip opening displacement model (CTOD-Model) was utilized to estimate the fracture toughness using a three-point bend specimen following ASTM-E-1290. After taking load-displacement information from the ANSYS SOFTWARE and using it in the (CTOD-Model), the critical value for crack tip opening displacement will be determined using the elastic and plastic components, which are separated into two sections, respectively. The Dug Dual Model has been used to estimate the elastic component, and the Plastic Hinge Model will be used to estimate the plastic component. The fracture toughness value derived from this particular study is highly accurate as a result. Additionally, the CTOD-Model is used to evaluate fracture toughness utilizing the analysis of the non-linear three-dimensional finite element model following ASTM E-1290, and it yields great results for the output load-displacement data from ANSYS with high accuracy. The relation between load and displacement is linear, indicating that no or little plastic deformation occurs in the elements used in this program.

Madyira and Nyemba, (2020) [17] study of the effect of WEDM on the microstructure and fracture toughness of Ti6Al4V. Using compact tension CT specimen was to measure the fracture toughness while microstructural changes were studied using an optical microscope. Instead of introducing the pre-crack by the recommended fatigue cycling, WEDM was used. Obtained results indicated a slight decrease in fracture toughness compared to that reported in the literature. In addition, it can also be concluded that WEDM can be used as an alternative to fatigue pre-cracking in fracture toughness testing of Ti6Al4V.

2. Non-Linear Elastic-Plastic Fracture Mechanics (EPFM)

Elastic-Plastic Fracture Mechanics applies to materials that exhibit time-independent, plastic deformation. There are two elastic-plastic parameters that describe crack-tip conditions in elastic-plastic material, those are crack tip-opening displacement (CTOD) and J-Contour Integral.

-Crack tip opening displacement (CTOD)

This approach applies in both elastic and elastic-plastic conditions. CTOD method has the advantage of being able to measure CTOD values across the whole plane-strain, elastic-plastic, and fully plastic behavior regions, whereas K_{IC} values can only be measured in the plane-strain region or approximated in the initial stages of the elastic-plastic region [18].

In the current study, CTOD-Model will be used as a measure of fracture toughness, where it was from the type of ductile fracture. CTOD-Model is separated into two components, the elastic component & plastic component[7].

The elastic component of CTOD can estimate using Dug dual Model which has derived from the stress intensity factor K_I while the plastic component is only obtained from the plastic hinge model by converting the crack mouth opening displacement CMOD into CTOD using relationships of

similar triangles. This model will be used in the current study to predict fracture toughness value. CTOD represents a measure of the opening displacement mode of the crack face. Several values of this parameter can be calculated from the load-displacement records related to maximum load condition, first pop-in at brittle crack extension, and the onset of stable crack extension [19].

3. Methodology

3.1 Measurement of fracture toughness (critical CTOD)

According to the ASTM standard E 1290-02[20] the critical crack tip opening displacement during the loading consists of elastic (δ_{el}) and plastic (δ_{pl}) part, given by Eq.(1) [[7],[5],[9]].

Critical CTOD = Elastic CTOD + Plastic CTOD

$$\delta_C = \delta_{el} + \delta_{pl} \quad (1)$$

3.1. A Calculation for the elastic part (δ_{el})

The elastic part is calculated by using a standard equation for plane stress condition.

$$\delta_{el} = \frac{K_I{}^2}{mE\sigma_y} \quad (2)$$

m =1 for plane stress m=2 for plane strain where elastic modulus E and yield strength (S_y) are the mechanical properties. The theoretical stress intensity factor K_I for the CT specimens can be derived from Eq. (3)

$$K = \frac{P_Q}{\sqrt{BB_N}\sqrt{W}} f\left[\frac{a}{w}\right] \quad (3)$$

The value of P_Q is equal to P_c, load at crack initiation, B is the thickness of the specimen, W is the width of the specimen and

$$f\left[\frac{a}{w}\right] = \frac{\left(2+\frac{a}{w}\right)\left[0.886+4.64\frac{a}{w}-13.32\left(\frac{a}{w}\right)^2+14.72\left(\frac{a}{w}\right)^3-5.6\left(\frac{a}{w}\right)^4\right]}{\left(1-\frac{a}{w}\right)^{\frac{3}{2}}}$$

The experimental stress intensity factor K_I for the CT specimens can be derived from Eq. (4) [14].

$$K_I = (CMOD\ \sigma_y\ E)^{1/2} \quad (4)$$

3.1. B Calculation for the plastic part (δ_{pl})

In general, the plastic CTOD (δ_{pl}) is determined by using the plastic hinge method (PHM). This method assumes a linear relation between plastic load-line displacement (V_{pl}) and plastic CTOD (δ_{pl}). The plastic CTOD (δ_{pl}) is determined by assuming that the unbroken ligament works like an plastic hinge with its center (apparent axis of rotation) at a distance ($r_{pl}b$) from the crack tip. The plastic CTOD is found using Eq. (5) and shown in Fig.1A.

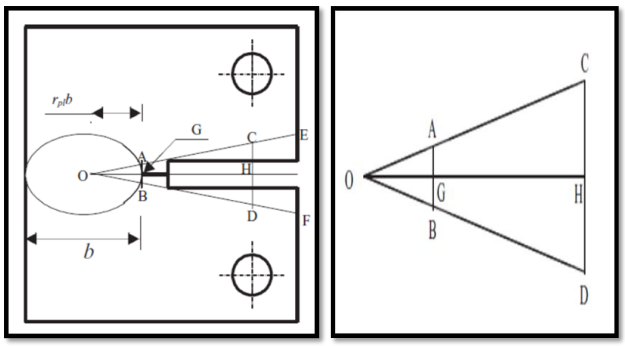

Fig.1 (A) plastic hinge model of stander compact tension, (B) crack-tip and load-line displacement geometry at crack initiation[7].

Referring to Fig.1 (a) and (b):
O = the apparent axis of rotation
G = crack tip
AB = the plastic part of the CTOD (δ_{pl})
CD = the plastic load-line displacement (V_{pl})
GH = the initial crack length (a)
OG = $r_{pl}b$
r_{pl} = the plastic rotational factor b = the ligament length
From properties of the similarity of triangle Fig.1 (A)

$$\frac{AB}{CD} = \frac{OG}{(OG+GH)} \quad (5)$$

$$\frac{\delta_{pl}}{V_{pl}} = \frac{r_{pl}b}{(r_{pl}b+a)} \quad (6)$$

where r_{pl} is a plastic rotational factor (PRF), V_{pl} is a plastic load line displacement and b is an unbroken ligament length. The value of PRF is given by Eq.7.

$$r_{pl} = \frac{(1+\alpha)}{2} \quad (7)$$

$$\alpha = \left[\left(\frac{2a}{b}\right)^2 + \left(\frac{4a}{b}\right) + 2\right]^{1/2} - \left[\left(\frac{2a}{b}\right) + 1\right] \quad (8)$$

Eq.9 is used to find equivalent fracture toughness:

$$K_Q = (\delta_C E S_y)^{0.5} \quad (9)$$

While the plastic component of the crack tip opening displacement δ_{pl} will be estimated by the plastic hinge model as shown in Fig.1, after converting the clip gauge displacement (V_p) which can be extracted from the load Crack Mouth Opening the displacement curve as shown in Fig.2 and entering (V_p) in Eq.6 in order to obtain δ_{pl}.

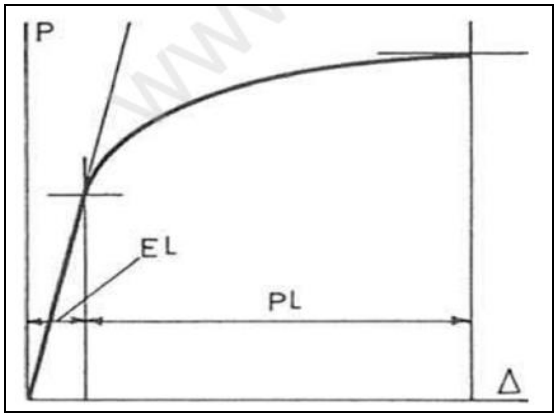

Fig.2 The curve of load line displacement [21].

3.2 Thickness Effect on ($CTOD_C$) Fracture Toughness

For a component with a crack and external load, stress intensity factor K_I (take mode I crack as an example) is a mechanics parameter to describe the stress field in a crack tip. K_I would increase if external loading increases. When K_I increases to a critical value, the crack in the component begins to grow. This critical value is called fracture toughness K_C or K_{IC}, which represents the material's ability to resist unstable propagation of the crack. Fracture toughness K_C or K_{IC} is an inherent attribute of a material. The difference is that K_C is fracture toughness under plane stress state, which would be influenced by the thickness of the plate or test specimen. When specimen thickness increases, fracture toughness tends to be a stable and lowest value, which would not be influenced by thickness. This value is called K_{IC} or plane strain fracture toughness. K_{IC} is the real material constant, which reflects the material' s ability to prevent crack extension[4].

4. Experiment

4.1 Aim of the Experiments

- **A.** Studying of mechanical and microstructure properties of the material selected.
- **B.** Determined the crack mouth opening displacement (CMOD) in various load applied by using displacement transducers (data logger device) connecting with a computer to the tensile machine.
- **C.** Determine the critical crack tip opening displacement CTOD experimentally, (CTOD) is found with the help of plastic hinge model (PHM) method.
- **D.** Study the effect of variation of thickness on the plane stress fracture toughness.
- **E.** Study the effect of WEDM on the fracture toughness of low carbon steel, and also required to establish if the use of WEDM to introduce pre-cracks in compact tension specimens that are used to measure fracture toughness is a viable substitute for the more time-consuming fatigue pre-cracking.

4.2 Material

A sample of ASTM A-36 low steel was purchased from a local market. The chemical composition of the mild steel sample was determined as given in Table 2. Standard tensile specimens were made from ASTM A-36 low steel samples using a lathe machine.

low carbon steel that is used in this investigation with a thickness of (8,10, and15)mm is used as a base metal for the experimental work. The plate was machined and cleaned to remove dirt and oxides in the workshop of the College of the Engineering / University of Basrah to get on the required sample for the required experimental tests.

•Applications:

Low steel can be used to create products across a wide variety of industries, making it one of the most popularly used types of steel. Uses for mild steel include structural steel, signs, automobiles, furniture, fencing, roods, valves, gears, crankshafts, connecting rods, railway axles, and other components are made of it.

4.3 Mechanical properties

A) Tensile test

One of the most significant and commonly analyzed characteristics of materials is the ability to stand cracking under tensile stress. To determine the tensile strength, a computerized universal testing machine is used, and three tensile specimens are prepared using a lathe machine following the ASTM (E8/E8M-13a)[22] standard with all dimensions in mm shown in Fig .3. The specimen is placed in the tensile machine until the specimen is fractured as shown in Fig.4. The machine device of 600 KN capacities used in this test was " Instron Tensile Machine ", with fully controlled computer programming as shown in Fig.5.

In a tensile test, a specimen is fixed to the end of the grippers which is connected to the upper plate and lower plate of the Instron Tensile Machine.

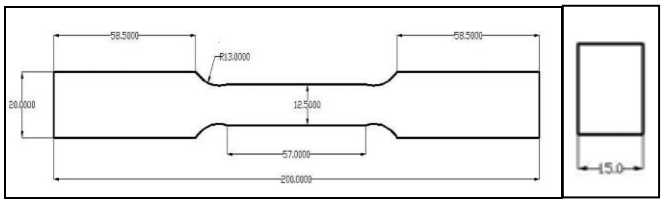

Fig.3 Diaminsionof tensile test specimens (all Daiminatsion in mm).

Fig.4 Tensile test specimens after a fracture.

Fig.5 INSTRON Tensile Test Machine.

To determine the material's ultimate tensile strength, a specimen is extended up to it is breaking point using a controlled system connected to the INSTRON Tensile Machine. During the experiment, the amount of force applied (F) and the sample elongation (L) is measured. Material characteristics are commonly described using the terms stress (force per unit area) and strain (change in length to the original length). The results are plotted on an XY chart as a stress vs. strain graph shown in Fig.6. The program placed on the PC connected to the tensile machine recorded all load and displacement data during the test. To assess the tensile properties of low-carbon steel, tensile tests were carried out as per ASTM (E8/E8M-13a) standards. Table .1 shows the best result obtained.

Table1. The mechanical properties of low-carbon steel.

Thickness (mm)	Yield stress (Mpa)	Ultimate tensile stress (Mpa)	Modulus Elasticity E (Gpa)	v
8,10,15	287.8	433.6	200	0.3

Then stress-strain curve was drawn by Microsoft office excel 2010 as shown in Fig.6.

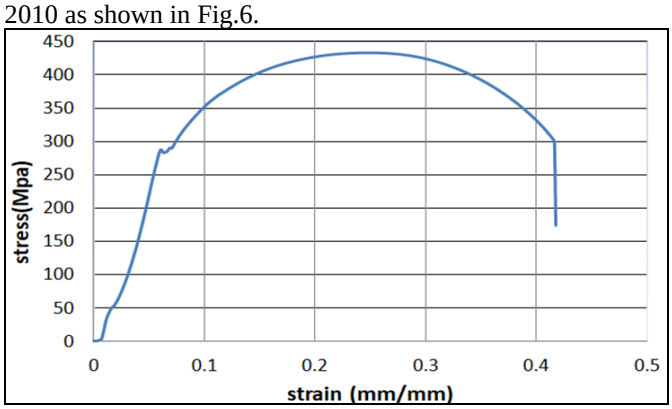

Fig.6 Stress-strain curve**.**

B) The chemical composition test

This test aims to estimate the required chemical properties of the selected material. One small specimen plate of carbon steel shown in Fig.7 (A) was analyzed to examine it is a chemical composition by using the Spectrometer device as shown in Fig.7 (B).

Fig.7 (A) Small piece of metal, (B) Spectrometer device**.**

The chemical composition of the material as presented in the test is shown in Table 2.

Table 2. Chemical composition of mild carbon steel.

Element	**C**	**Si**	**Mn**	**P**	**S**	**Cr**	**Fe**
Percentage %	0.097	0.234	0.69	0.003	0.002	0.011	98.8

4.4 Specimen preparation

The geometry of the CT specimen used in the present work is as per the recommended design in ASTM standard E 399 - 13[23]. Specimens are fabricated by using: a wire-cut electric discharge machine (WEDM) to maintain the exact relationship between all the dimensions. Fig.8 shows the specimen dimensions, and Figs. (9, and10) show a prepared specimen for the fracture test. In the present study, pre-cracking is done by using a molybdenum wire cut WEDM operation with a notch radius (ρ) of 0.18 mm. The dimensions of the specimen are thickness (B) (8, 10, and 15) mm, Width (W) = 30mm, crack length (a) = 22.5mm, notch length = 1.3 mm, (ρ) = 0.18mm.

Water and oil were used as the dielectric, and a specimen was machined to have the specified dimensions and configuration of the compact tension. There were three stages to the preparation using the WEDM machine. In the first stage, a 0.18 mm diameter wire was used to the specimen's profile according to the dimensions. Following that, a 0.18 mm diameter wire was used to introduce the (1.3mm) pre-crack instead of fatigue pre-crack. The two holes are prepared with a 9.8 mm diameter by drill press shown in Fig.10. After that, the specimens were separated from the main bar in Fig.9.

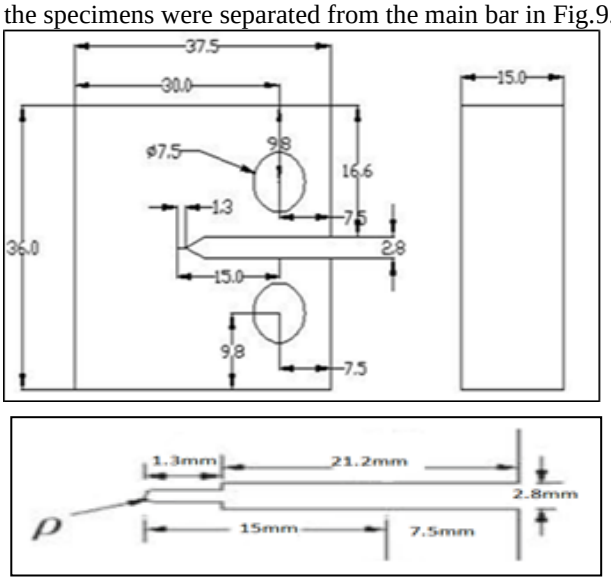

Fig.8 specimen dimensions following ASTM E 399-13 all dimensions in (mm).

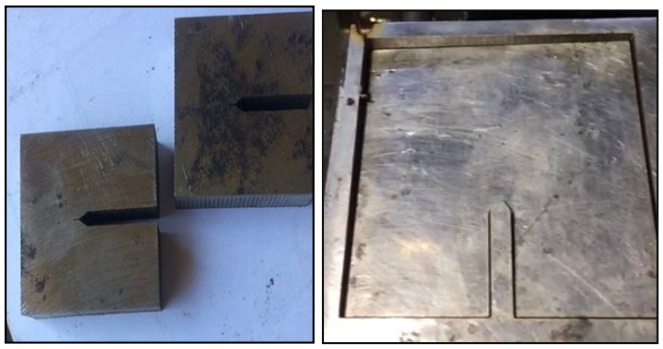

Fig.9 Steps of preparation of CT specimens.

Fig.10 Using the drill press to have the hole compact tension CT specimen.

5.5 Pre-cracking procedure

Fracture mechanics approach is important for all mechanical and civil projects that might involve cracks in metallic materials.

The aim of pre-cracking is to simulate a real crack in a structure, so it should be narrow and deep enough to avoid the effects of the machined notch. The fracture toughness test is performed after the specimen is pre-cracking. For the notch it is recommended to use electric discharge machining (EDM), as it does not affect the region around the notch and offers an easier way to start a crack by fatigue; depending on the material the pre-cracking procedure could be avoided [11].

The theory of fracture mechanics applies to cracks that are infinitely sharp before being loaded, while laboratory specimens will always fall short of this ideal, it is important to initiate cracks that are acute enough to use cyclic loading as the most efficient approach to creating such a crack. The fatigue crack must be introduced in such a way that it has no serious effect on the toughness value being tested. Because cyclic loading produces a finite-radius crack with a small plastic zone at the tip, but because this technique is costly and time-consuming, we use the WEDM to introduce this crack in the current work seen in Fig. 11

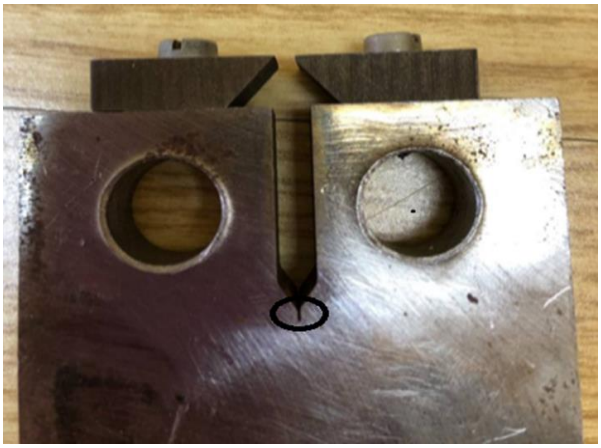

Fig.11 Pre-cracking by WEDM.

5.6 Side grooving

On each side of the specimen, the side grooving was machined to maintain a notch angle of 60° and a depth of nearly 1.5 mm into the sidewalls of specimens seen in Fig. 12. The primary goal of the side grooving is to ensure the crack front is straight during a test. Because the material towards the outside surfaces is in a state of low-stress triaxiality a specimen without side grooves is subject to crack tunneling and shear lip formation. Side grooves remove the low triaxiality zone, resulting in relatively straight crack fronts if done correctly.

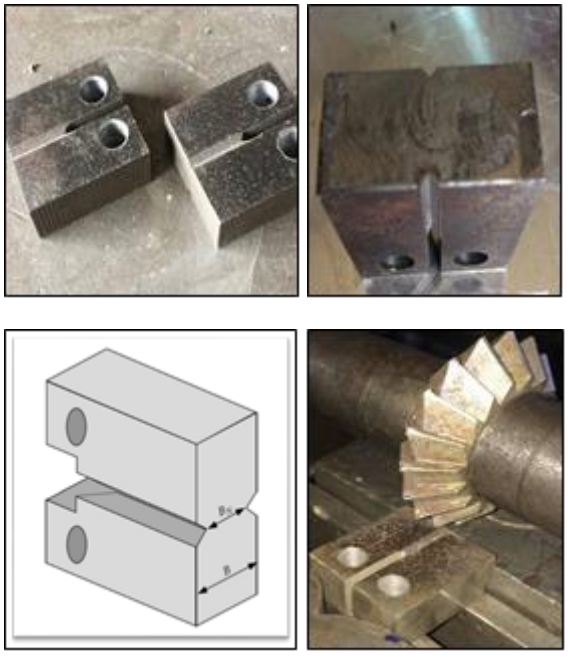

Fig.12 Side grooving.

5.7 Fixtures and Knife Blocks

The UB-5A Clip is a type of Displacement Transducers (clip gauge) that conforms to ASTM specifications shown in Fig.13. Knifes block structure for staffing the offset clip gauge is designed to conform to ASTM-E 399-13 standards for measuring the CMOD [displacement transducer] is shown in Fig.16. Figs. 14 and 15 are from the protocol for designing the knife blocks to contact the clip gauge for the measured CMOD. Fig.14 shows the rotation shape in the clip gauge during the run operation test rather than linear because the

angle value for the knife block edge is 60° for contact with the clip gauge edge. Knife blocks may be separate pieces affixed to the specimen as shown in Fig. 16.

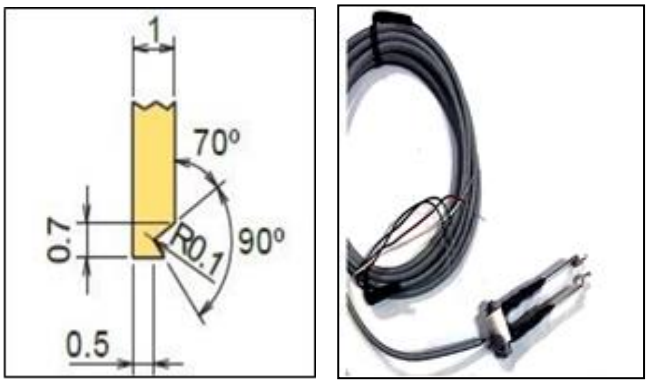

(A) (B)

Fig.13 (A) Received CMOD notch details[14], (B) The UB-5A Clip type.

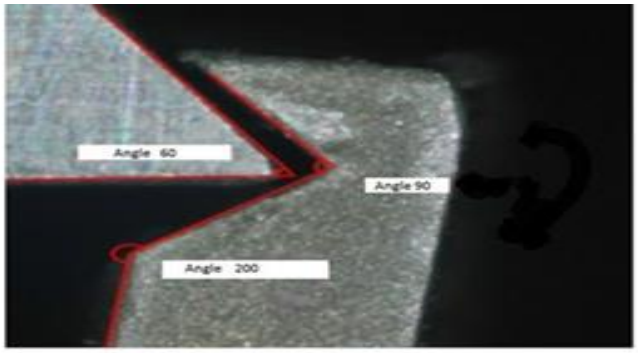

Fig.14 As specified 60° knife edge. The near-planer contact resulted in the relative motion of the contact point with the rotation of the knife edge[14].

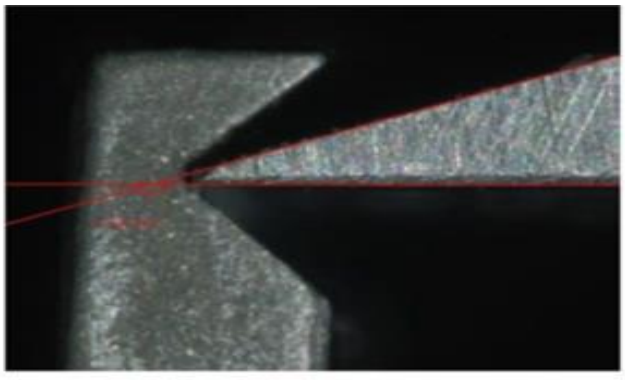

Fig.15 Sharpened knife edge design decreased the relative motion of the contact point during the rotation. Note that the termination of the knife edges was left at 60° [14].

Fig.16 Attachable knife-edge design.

This design features a knife-edge spacing of 5 mm. The effective gauge length is established by the points of contact between the screw and the hole threads. between the screw and the hole threads.

After that, we have complete specimens as shown in Fig.17.

Fig.17 CT specimens.

A loading clevis suitable for testing standard compact CT specimen the size, proportions of the clevis shown in Fig. 18 according to ASTM-E399-13 are all scaled to specimens with *W/B* = 2. Both ends of the specimen are held in the clevis and loaded through pins to allow rotation of the specimen during testing. The clevis holes are provided with small flats on the loading surfaces to provide rolling contact, thereby minimizing friction effects.

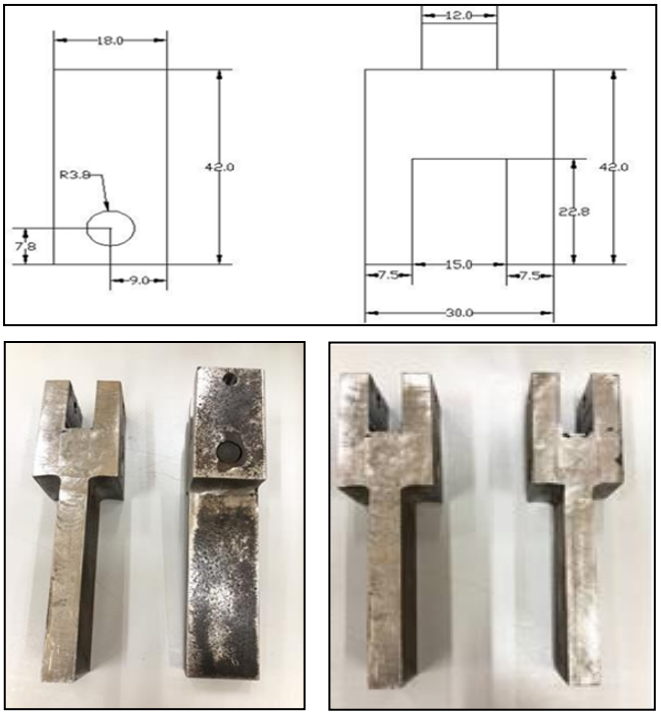

Fig.18 Loading clevis (all dimensions in mm).

5.8 Experimental setup

The test is carried out using a 100kN Universal Testing Machine. The experimental setup is shown in Figs. (19, and 20), the sample after reach to the critical load P_C shown in Fig.21.

A strain rate of 0.5mm/min was used for the fracture test. CMOD gauge is used to measure load-line displacement. Instead of CMOD, a load line displacement is measured. This is because of the smaller size of the specimens.

Fig.19 100kN Universal Testing Machine.

Fig.20 Tensile Test Machine and Test setup for CT type specimen.

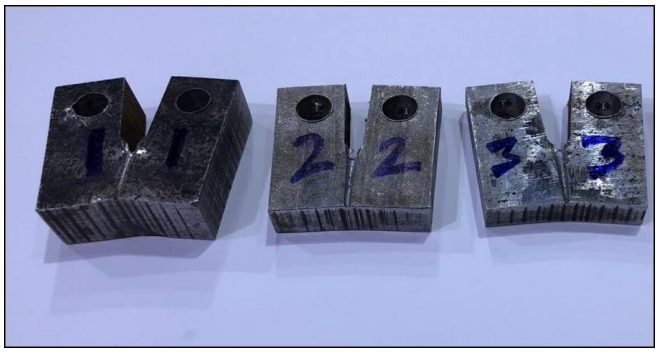

Fig.21 Specimens during the test, and after crack initiation.

6. Result and discussion

6.1 Critical load Results

The specimen was loaded under tension at the same time as the tensile operation. The data were recorded when the metal specimen was loaded into a 100KN tensile machine, the load was recorded from the program placed on the P_C connected to the tensile machine but the CMOD recorded from the displacement transducer during the load's amount difference in the same time at the room temperature as shown in Fig.22 and data as indicated in Table 3.

Fig.22 PC and displacement transducer.

Table3. Load –CMOD for all thicknesses of low (mild) carbon steel.

No	Load (KN)	CMOD		
		15mm	10mm	8mm
1	0	0	0	0
2	0.5	0.009	0.022	0.037
3	1	0.018	0.045	0.052
4	1.5	0.025	0.069	0.088
5	2	0.033	0.087	0.120
6	2.5	0.041	0.109	0.163
7	3	0.049	0.0136	0.215
8	3.5	0.060	0.163	0.274
9	4	0.071	0.194	0.349
10	4.5	0.081	0.224	0.437
11	5	0.093	0.253	0.545
12	5.5	0.105	0.286	0.678
13	6	0.117	0.320	0.909
14	6.5	0.130	0.355	1.384
15	7	0.142	0.405	1.959
16	7.5	0.156	0.481	3.091
17	8	0.170	0.792	3.511
18	8.5	0.186	1.105	0
19	9	0.203	1.434	0
20	9.5	0.219	1.826	0
21	10	0.238	2.330	0
22	10.5	0.259	2.943	0
23	11	0.281	3.624	0
24	11.5	0.310	3.851	0
25	12	0.355	0	0
26	12.5	0.406	0	0
27	13	0.508	0	0
28	13.5	0.701	0	0
29	14	0.992	0	0
30	14.5	1.264	0	0
31	15	1.532	0	0
32	15.5	1.813	0	0
33	16	2.11	0	0
34	16.5	2.469	0	0
35	17	2.905	0	0
36	17.5	3.511	0	0
37	17.88	3.794	0	0

Table 4. Maximum load (load for crack initiation) for all thickness

No	Thickness (mm)	Maximum load of fracture (KN)
1	8	8
2	10	11.5
4	15	17.88

The load vs. CMOD (Crack Mouth Opening Displacement) graphic is displayed in Fig.23. The curve shows normal behavior, showing a linear pattern during the initial loading stage and non-linear in a second stage with significant CMOD increases but a low load increase**.**

The fracture tests were carried out using an Instron universal testing machine with a loading rate corresponding to the constant crack head displacement of 0.5 mm/min at room temperature. During such tests, the magnitude of load P and load line displacement V were recorded together with time. It was observed that the load dropped at a particular instant when surface cracks were initiated.

At that instance time, the loading of a specimen was discontinued and the specimen was taken out for subsequent measurement of CTOD and analysis of alternate fracture criteria. A typical load–load line displacement plot is shown in Fig.23. It is observed that the load continuously increases till a Pc value, however, the rate of increment of load just before the critical load is very low as compared with the earlier portion of the plot. The rate of increment of load continues to decrease and as soon as the surface crack initiates, the load drop**s.**

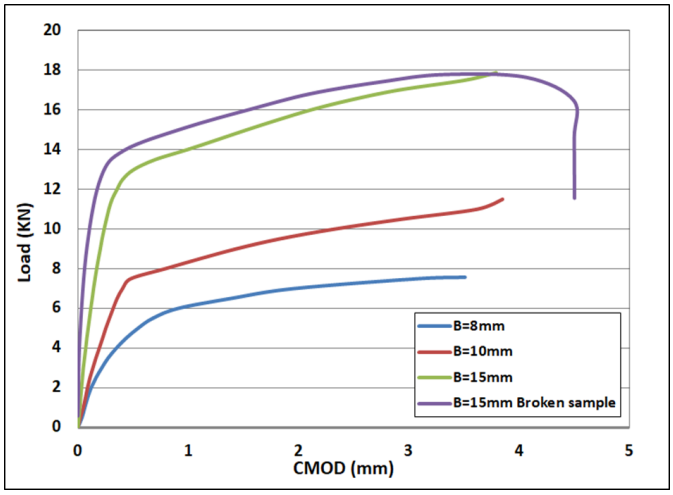

Fig.23 Load - CMOD for low carbon steel with (8, 10 and15) thickness.

6.2. Theoretical Stress Intensity Factor K_I

In order to study the effect of load on stress intensity factor, three thicknesses were selected, Stress Intensity Factor K_I of low carbon steel with a thickness (8, 10, and 15) mm that determined in the linear elastic region as calculated theoretically using Eq.3. Table5 shows the values of theoretical stress intensity factor K_I in the linear elastic region for low carbon steel with 8mm thickness (3.450) to (31.047) but in thickness 10 mm the stress intensity factor changing from (2.760mm) to (35.877) and in 15 mm thickness K_I between (1.840) to (42.315) Mpa √m.

Table 5. Show the theoretical stress intensity factor K_I for low-carbon steel metal specimen (B=8, 10, and 15mm).

Theoretical K_I , MPa√m			
Load (KN)	8 mm	10 mm	15 mm
0	0	0	0
0.5	3.450	2.760	1.840
1	6.810	5.520	3.680
1.5	10.349	8.279	5.519
2	13.799	11.039	7.360
2.5	17.248	13.799	9.199
3	20.698	16.558	11.039
3.5	24.148	19.318	12.879
4	27.597	22.078	14.718
4.5	31.047	24.838	16.558
5		27.597	18.398
5.5		30.357	20.238
6		33.117	22.078
6.5		35.877	23.917
7			25.757
7.5			27.597
8			29.437
8.5			31.277
9			33.116
9.5			34.956
10			36.796
10.5			38.636
11			40.476
11.5			42.315

6.3. Experimental Stress Intensity Factor K_I

Table 6 shows the value of experimental stress intensity factor K_I for the linear elastic region for Low carbon steel values as calculated using Eq.(4)[9]. Tables 6 show the measurement of stress intensity factor K_I of the mild carbon steel specimens tested under the Mode-I loading condition. When the applied load of 0.5 kN was on the specimens, the 8mm specimen thickness gave a stress intensity factor of 46.149 MPa√m while the 10 mm thickness specimens is 35.585 MPa√m, and in 15mm thickness specimens is 22.760 MPa√m.

Table 6. Shows the Experimental results of the stress intensity factor (SIF) for thickness.

Load	Stress intensity factor K_I (MPa$\sqrt{m}$)		
	8(mm)	10(mm)	15(mm)
0	0	0	0
0.5	46.149	35.585	22.760
1	59.739	53.585	32.188
1.5	71.171	63.021	37.934
2	83.110	70.765	43.583
2.5	96.862	79.209	48.579
3	111.503	88.477	53.108
3.5	125.584	96.862	58.767
4	141.734	105.672	63.928

4.5	158.599	113.549	68.281
5		120.676	73.165
5.5		128.305	77.742
6		135.717	82.064
6.5		142.947	86.503
7		152.682	90.408
7.5			94.759
8			98.920
8.5			103.471
9			108.096
9.5			112.275
10			117.044
10.5			122.098
11			127.178
11.5			133.58

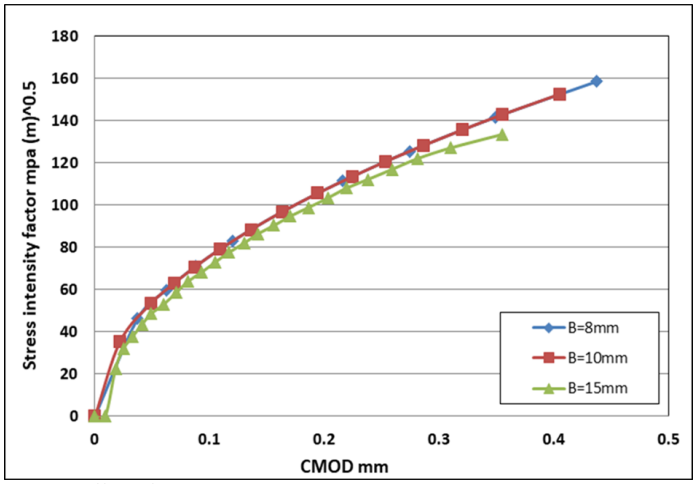

Fig 24 Effect of crack mouth opening displacement on experimental stress intensity factor KI in linear region for each thickness.

6.4 Comparison between experimental and theoretical stress intensity factor K_I

The max load needed to cause cracks were similar to the experimental values. Figs. (24, 25, and 26) show a comparison of the experimental and theoretical stress results in the elastic region.

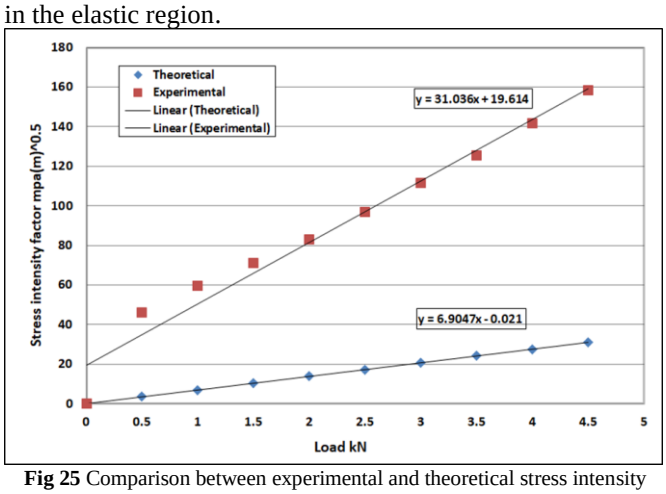

Fig 25 Comparison between experimental and theoretical stress intensity factor K_I for 8mm thickness.

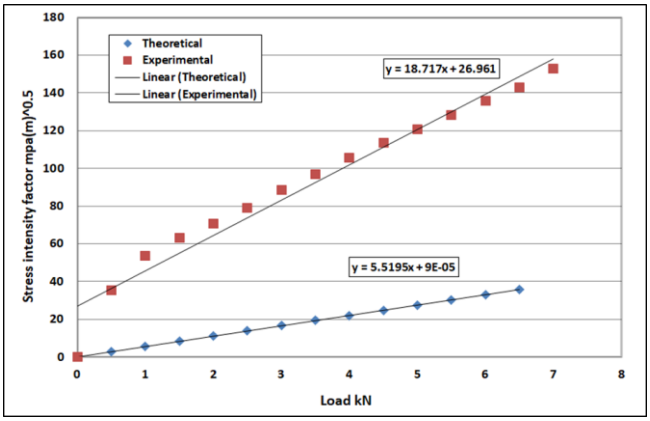

Fig 26 Comparison between experimental and theoretical stress intensity factor K_I for 10 mm thickness.

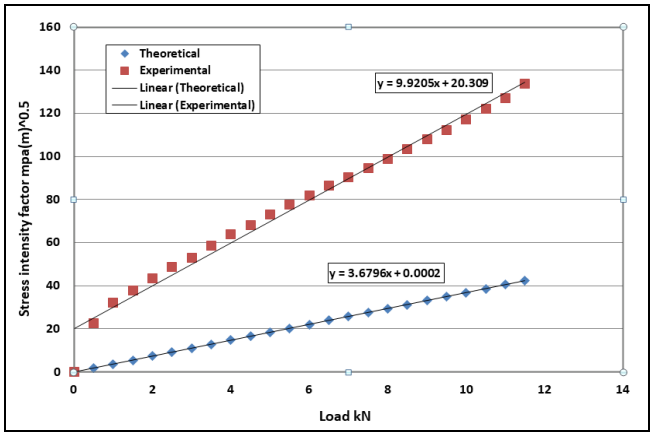

Fig 27 Comparison between experimental and theoretical stress intensity factor K_I for 10 mm thickness.

6.5. Calculation of the critical CTOD

The critical crack tip opening displacement CTOD for low carbon steel is determined according to the ASTM standard E1290-02[20], that the critical crack tip opening displacement during the loading consists of two parts; elastic $(\delta_t)_{el}$. and plastic $(\delta_t)_{pl}$. parts, Fig.23 represented this two-part and critical load for all thickness specimens. The linear stress intensity factor K_I is calculated according to Eq.3 and listed in Table 5. The critical stress intensity factor K_I is calculated in critical load shown in Table 7.

Table 7. Show the critical stress intensity factor (K_I) for all thicknesses of low-carbon steel metal specimens.

Thickness B (mm)	Specimen thickness between the roots of the side grooves B_N (mm)	Critical load P_C (KN)	Linear stress intensity factor K_I (Mpa$\sqrt{m}$)
8	7	7.5	55.317
10	9	11.5	66.907
15	14.5	17.88	66.917

6.5. (A) Elastic crack tip opening displacement $(\delta_t)_{el}$ calculation:

A standard method is used to calculate the elastic portion according to Eq.2 and listed in Table 8

Table 8 shows the experimental results of the Elastic CTOD $(\delta_t)_{el}$ for each thickness of low-carbon steel metal specimens.

Thickness B (mm)	Elastic CTOD $(\delta_t)_{el}$ (mm)
8	0.0531
10	0.0778
15	0.0778

6.5. (B) Plastic crack tip opening displacement $(\delta_t)_{Pl}$. calculation:

The plastic portion of $CTOD_C$ $(\delta_t)_{pl}$. is determined according to Eq.6 by considering that the un-cracked ligament serves as a plastic hinge, with its center ($r_{pl}b$) from the crack tip.

Table 9. Experimental results of the Plastic CTOD $(\delta_t)_{Pl}$ for each thickness.

thickness B (mm)	ligament length b (mm)	plastic rotational factor(r_{pl}) (mm)	α	plastic load-line displacement	plastic crack tip opening displacement $(\delta_t)_{pl.}$ (mm)
8	14	0.578	0.155	2.911	0.978
10	14.2	0.579	0.157	3.201	1.096
15	14	0.578	0.155	3.344	1.123

The value (V_{pl}) is taken from Fig.23. With the help of Eq.1, 2, and 6, the essential $CTOD_C$ value is computed for various thicknesses. Because the stress singularity in general yielding fracture mechanics (GYFM) is an incorrect concept, the value of the critical stress intensity factor is denoted here as an equivalent fracture toughness value K_Q rather than K_c. Eq.9 is used to obtain equivalent fracture toughness.

Table 10. Experimental results of the critical $CTOD_C$ and fracture toughness for all thicknesses.

Thickness B (mm)	$CTOD_C$ (mm)	Equivalent fracture toughness K_Q MPa$\sqrt{m}$
8	1.038	344.277
10	1.174	366.137
15	1.201	370.323

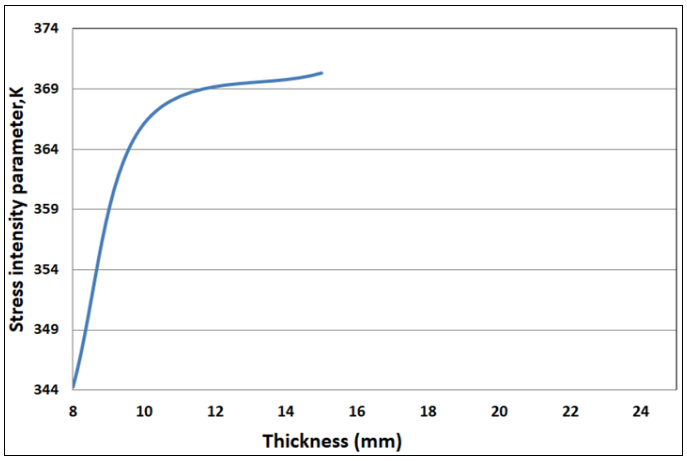

Fig.28 Effect of plate thickness on fracture toughness at the crack tip.

The results in Fig.28 reveal of K_Q is increased with thickness, the reason for this behavior is that in reducing the thickness of the plate, the plastic zone around the crack tip will be increased which leads to the reduction in the value of K_Q.

7. Conclusion and Discussion

In this work, the stress intensity factor K_I characterization was realized in structural steel low carbon steel according to ASTM E-399-12 of linear elastic region fracture mechanics. Prediction of stress intensity factor and crack mouth opening displacement for standard test CT specimens has been carried out experimental.

Based on the results obtained, the following conclusions can be made:

1. The thickness effect refers to the impact of the plastic zone at the crack tip on the stress intensity factor. The thinner the specimen, the bigger the plastic zone at the fracture tip leading to a high stress intensity factor at the fracture tip. The thick specimen, on the other hand, has a low stress intensity factor around the crack tip.
2. The stress intensity factor, K_I, increases with increased loading in the elastic region.
3. WEDM caused a heat-affected zone HAZ on the material's surface, which was more severe in the crack tip region, this is the reason for the increased stress in the experimental results and the high rate of error between experimental and theoretical values.
4. Fracture toughness varies with thickness; the explanation for this behavior is that as the thickness of the plate is increase, the plastic zone around the fracture tip decrease, causing the value of K_Q to increase.

Nomenclature

Symbol	Description	SI Unit
K_Q	The Conditional Stress Intensity Factor	$Mpam^{1/2}$
K_I	Stress Intensity Factor For a Mode I Crack	$MPam^{1/2}$
K_{IC}	Plain Stress Fracture Toughness	$Mpam^{1/2}$
K_C	Plain Strain Fracture Toughness	$Mpam^{1/2}$
CMOD	Crack Mouth Opening Displacement	mm
a	Crack length	mm
ASTM	American Society for Testing and Materials	m,N,pa
SIF	Stress intensity factor	$MPam^{1/2}$
W	width	mm
B	Thickness	mm
CT	Compact Tension	----
P_Q	Conditional Fracture Load	KN
B_N	Specimen thickness between the roots of the side grooves	mm
EPFM	Elastic-Plastic Fracture Mechanic	----
E	Modulus of Elasticity	Mpa
σ_{ys}	yield stress	Mpa
XFEM	Extended Finite Element	----

	Method	
PHM	Plastic Hinge Model	----
F(a/W)	polynomial based on the crack length divided by the width	---
V	Poisson's ratio	---
FEA	Finite Element Analysis	---
WEDM	Eire Electric Discharge Machine	---
LEFM	Linear Elastic Fracture Mechanics	---
SENB	Single Edge Notch Bending	----
CTOD	Crack Tip Opening Displacement	mm
$CTOD_C$	Critical Crack Tip Opening Displacement	mm
$CTOD_{Pl}$	Plastic Crack Tip Opening Displacement	mm
$CTOD_{El}$	Elastic Crack Tip Opening Displacement	mm
EDD	Extra Deep Drawn	----
EDM	Electric Discharge Machine	
CFOA	Crack Flank Opening Angle	----
COD	Crack Opening Displacement	$Mpam^{1/2}$
K_{max}	Maximum Fracture Toughness	$Mpam^{1/2}$
SECT	Single Edge Crack Tension	----
δ_{el}	Elastic crack tip opening displacement	mm
δ_{pl}	Plastic crack tip opening displacement	mm
b	ligament length	mm
r_{bl}	plastic rotational factor	mm
α	The dimensional parameter influenced by the specimen and crack geometries	----
V_{PL}	plastic load-line displacement	mm
ρ	notch radius	mm

References:

[1] Hassanein Kh, "Problems by Using Experimental and Crack Propagation in Plane Stress Extended Finite Element Method (XFEM).", Ph.D Thesis, Mechanical Engineering Department, College of Engineering, University of Basrah, , 2015.

[2] S.S. Nama and R.M. Laftah, "Investigation of Stress Intensity Factor for Corrugated Plates with Different Profiles Using Extended Finite Element (XFEM)," Basrah Journal for Engineering Sciences, vol. 18, no. 1, pp. 1–9, 2018.

[3] WeeLiam Kh., "CRACK TIP OPENING DISPLACEMENT (CTOD) IN SINGLE EDGE NOTCHED BEND (SEN(B))," Ph.D Thesis, Mechanical Engineering Department, College of Engineering, Brunel University of London, 2018.

[4] H. Zhang, H. Zhang, X. Zhao, Y. Wang, and N. Li, "Study of Thickness Effect on Fracture Toughness of High Grade Pipeline Steel," MATEC Web of Conferences., vol. 67, pp. 4–11, 2016.

[5] V. V. Chaudhari, D. M. Kulkarni, and R. Prakash, "Study of influence of notch root radius on fracture behaviour of extra deep drawn steel sheets," Fatigue & Fracture of Engineering Materials & Structures, vol. 32, no. 12, pp. 975–986, 2009.

[6] T. L. Panontin, A. Makino, and J. F. Williams, "Crack tip opening displacement estimation formulae for C(T) specimens," Engineering Fracture Mechanics, vol. 67, no. 3, pp. 293–301, 2000.

[7] D. Kulkarni, R. Prakash ,and A. KUMAR, "Experimental and finite element analysis of fracture criterion in general yielding fracture mechanics," sadhan, vol. 27, no. December, pp. 631–642, 2002.

[8] S. K. Kudari and K. G. Kodancha, "On the relationship between J-integral and CTOD for CT and SENB specimens," Frat. ed Integrità Strutt., vol. 2, no. 6, pp. 3–10, 2008.

[9] D. Kulkarni, V. Chaudhari, R. Prakash, and A. Kumar, "Effect of thickness on fracture criterion in general yielding fracture mechanics," Int. J. Fract., vol. 151, no. 2, pp. 187–198, 2008.

[10] D. M. Madyira, "Effect of Wire EDM on microstructure and fracture toughness of 7075-T6511 aluminum alloy," Proceedings of the World Congress on Engineering, vol. 2218, pp. 1038–1042, 2015.

[11] J. Avila, V. Lima, C. Ruchert, P. Mei, and A. Ramirez, "Guide for recommended practices to perform crack tip opening displacement tests in high strength low alloy steels," Soldagem & Inspecao, vol. 21, no. 3, pp. 290–302, 2016.

[12] R. Soltysiak, D. Boroński, and M. Kotyk, "Experimental verification of the crack opening displacement using finite element method for CT specimens made of Ti6Al4V titanium alloy," AIP Conference Proceedings., vol. 1780, 2016.

[13] M. Heidarvand, N. Soltani, and F. Hajializadeh, "Experimental and numerical determination of critical stress intensity factor of aluminum curved thin sheets under tensile stress," Journal of Mechanical Science and Technology, vol. 31, no. 5, pp. 2185–2195, 2017.

[14] M. J. Abdulsada, "Experimental and Numerical Study of Mechanical Properties and Fracture Mechanics Analysis of AISI1010 Low Carbon Steel Welded Joints," M.Sc. Thesis, Mechanical Engineering Department, College of Engineering, University of Basrah, 2018.

[15] S. Ahamed, Roshan, and Shilpa, "EVOLUTION OF TENSILE AND FRACTURE TOUGHNESS PROPERTIES OF ALUMINUM-7075 ALLOY REINFORCED WITH ZIRCONIUM SILICATE (ZrSiO4) PARTICULATES Dr.," International Research Journal of Engineering and Technology (IRJET), vol. 07, no. 08, pp. 1314–1320, 2019.

[16] A. A. Nassar and E. G. Fayyad, "Linear and Non-Linear Stress Analysis for the Prediction of Fracture Toughness for Brittle and Ductile Material using ASTM E399 and ASTM E1290 By ANSYS Program package." Materials Science and Engineering, vol.579, 2019.

[17] D. M. Madyira and E. T. Akinlabi, "Effects of wire electrical discharge machining on fracture toughness of grade 5 titanium alloy," Proceedings of the World Congress on Engineering, vol. 2, no. March, pp. 1393–1398, 2014.

[18] A. E. Elwi and G. Y. Grondin, "Simulation of Crack Propagation in Steel Plate with Strain Softening Model," no. 266, 2006.

[19] C. al Kilicgil, "DEVELOPMENT OF A NEW

METHOD FOR MODE I FRACTURE TOUGHNESS TEST ON DISC TYPE ROCK SPECIMENS," La Soc, vol. 3, no. September, pp. 5–65, 2006.
[20] American Standard, "ASTM - E1290 Standard Test Method for Crack-Tip Opening Displacement (CTOD) Fracture," Astm, vol. 03, no. March, pp. 1–13, 2003.
[21] A. Shukla, Practical fracture mechanics in design, 2005.
[22] American Standard, "Standard Test Methods for Tension Testing of Metallic Materials" 2013.
[23] American Standard, "Standard Test Method for Linear-Elastic Plane-Strain Fracture Toughness K_{Ic}" 2013.